

**L-EDGE XANES MEASUREMENTS OF THE OXIDATION STATE OF TUNGSTEN IN IRON BEARING AND IRON FREE SILICATE GLASSES.** L. R. Danielson<sup>1,2</sup>, K. Richter<sup>2</sup>, S. Sutton<sup>3</sup>, M. Newville<sup>3</sup>, L. Le<sup>1,2</sup>, <sup>1</sup>Jacobs Sverdrup Co., Houston, TX 77058 United States (lisa.r.danielson@nasa.gov), <sup>2</sup>NASA JSC, 2101 NASA Road One, Houston, TX 77058 United States, <sup>3</sup>GSECARS University of Chicago, 9700 South Cass Avenue, Bldg. 434A, Argonne, IL 60439 United States.

**Introduction:** Tungsten is important in constraining core formation of the Earth because this element is a moderately siderophile element (depleted  $\sim 10$  relative to chondrites) and, as a member of the Hf-W isotopic system, it is useful in constraining the timing of core formation. A number of previous experimental studies have been carried out to determine the silicate solubility and metal-silicate partitioning behavior of W, including its concomitant oxidation state. However, results of previous studies (Fig. 1) are inconsistent on whether W occurs as  $W^{4+}$  or  $W^{6+}$ .

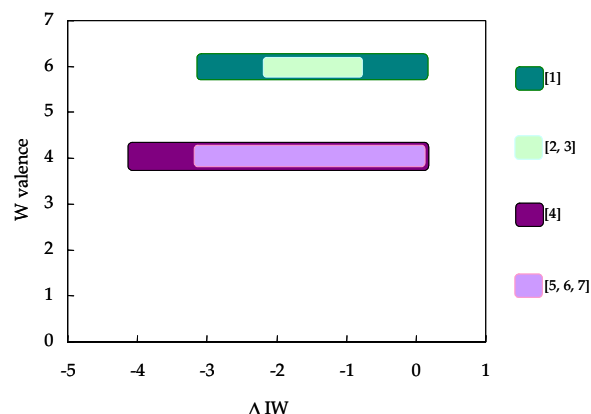


Figure 1. Comparison of W valence from previous results.

It is assumed that  $W^{4+}$  is the cation valence relevant to core formation [8]. Given the sensitivity to silicate composition of high valence cations [8], knowledge of the oxidation state of W over a wide range of  $fO_2$  is critical to understanding the oxidation state of the mantle and core formation processes. This study seeks to measure the W valence and change in valence state over the range of  $fO_2$  most relevant to core formation, around IW-2.

**Experiments:** Two compositions were used to determine the effects of iron content. Initial experiments, reported in [9] were conducted at 1300 °C, for durations of 24 to 96 hours and air or water quenched. One series was conducted using the An-Di eutectic, from QFM to IW-5 ( $\log fO_2$  -7.25 to -16. Experiments using an ankaramite starting composition were conducted from IW-1 to IW-5 ( $\log fO_2$  -11.75 to -16). Experiments were doped with 1wt% of  $WO_3$ . For both starting compositions, at IW-1, one set of experiments was doped with 1wt% of  $WO_2$ . Experiments at IW-2 and

above were conducted using a Re wire loop technique, while experiments below IW-2 were conducted in sealed silica tubes as in Fig. 2.

The most recent experiments reported herein expanded the  $fO_2$  range, from in air to IW-10 (ankaramite runs up to  $\log fO_2$  -0.4, CMAS runs down to  $\log fO_2$  -20) of the data set, and were designed to in an attempt to improve success with analyzable runs at low  $fO_2$ . Run duration was increased to 120 hours and all experiments were water quenched. Because the solubility of W decreases to  $\sim 100$  ppmw [4] at the low  $fO_2$  conditions of these experiments, amount of W as  $WO_3$  added was below 1000 ppmw.

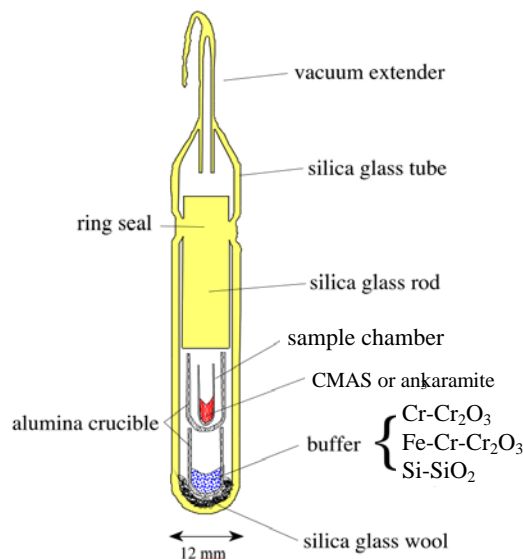


Figure 2. Schematic of sealed silica tube experiments conducted at lowest  $fO_2$ , below IW-2.

**Analytical:** A monochromatic X-ray beam from a Si(111) double crystal monochromator was focused onto the sample and the fluorescent X-ray yield was plotted as a function of incident X-ray energy (more detail can be found in [10]). The oxidation state of tungsten was inferred from the energy of the first peak in the LIII-edge derivative spectrum.  $WO_2$ ,  $WO_3$ ,  $FeWO_4$ ,  $CaWO_4$ , were used as standards.

**Results:** Results (Fig. 3 and 4) for both the iron-bearing and iron-free starting materials suggest that only  $W^{6+}$  is present from the most oxidized conditions to IW ( $\log fO_2$  -10.75). At IW, tungsten starts to exhibit mixed valence but is still dominated by  $W^{6+}$  for

ankaramite. At IW-2,  $W^{4+}$  becomes more abundant for ankaramite, but a definitive transition to  $W^{4+}$  below IW-2 has not been observed. CMAS has a lower W valence than ankaramite below IW, with the most reduced state observed being  $W^{4+}$ . These results suggest that  $W^{4+}$  would be dominant below IW-2.

Even with improved experimental technique focused on reducing the “nugget effect,” at IW-2 and below, metal exsolved from the silicate, complicating the analyses. Analyses in nugget free regions of the silicate portion of the experiments cluster around  $W^{5+}$ , while analyses in nugget-rich regions cluster around  $W^{2+}$ .

Four CMAS run products from Ertel [4] were also analyzed and shown for comparison in Fig. 4. These samples were reported as  $W^{4+}$ , from the slope of the W concentration vs.  $\log fO_2$  line. The Ertel run products are in good agreement with our CMAS run products, showing decreasing W valence with decreasing  $fO_2$ , but appear to be mixed  $W^{6+}$  and  $W^{4+}$  valence.

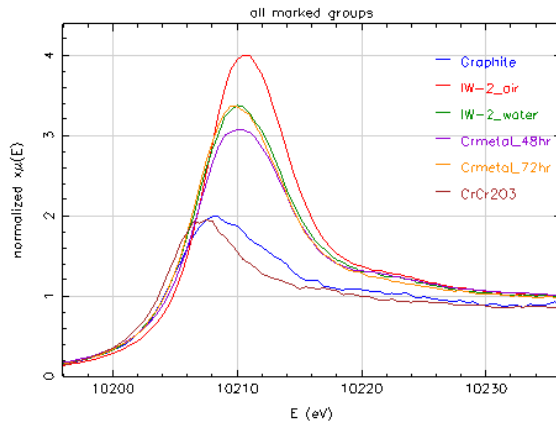


Figure 3. A sampling of results from some CMAS run product analyses (figure 4), showing range of W valence, from  $W^{6+}$  (IW+1 air quench, red line) to around  $W^{2+}$  (IW-5, using Cr-Cr<sub>2</sub>O<sub>3</sub> buffer, brick line). Data show differences between air (red line) and water quench (green line) at IW-2, with a 0.5+ reduction in W valence observed for a water quench. Other lines indicate a run in a graphite capsule, and runs using only Cr metal as a buffer.

**Discussion and Conclusions:** Both CMAS and ankaramite glasses show  $W^{6+}$  above IW and mixed valence below IW. The transition to  $W^{4+}$  only, appear to happen at or below IW-2 for iron free systems, but probably below IW-3 for iron bearing systems. Analyses of run products from previous experiments [4], support the observation the iron free transition to only  $W^{4+}$  occurs at or below IW-2.

The mixed states below IW-2 may result from analyses in which both silicate glass and exsolved W-bearing metal are present in the analytical volume in

varying proportions. This suggests if all W were dissolved in the silicate in a nugget free condition, W valence would be less than  $W^{5+}$  at lowest  $fO_2$ .

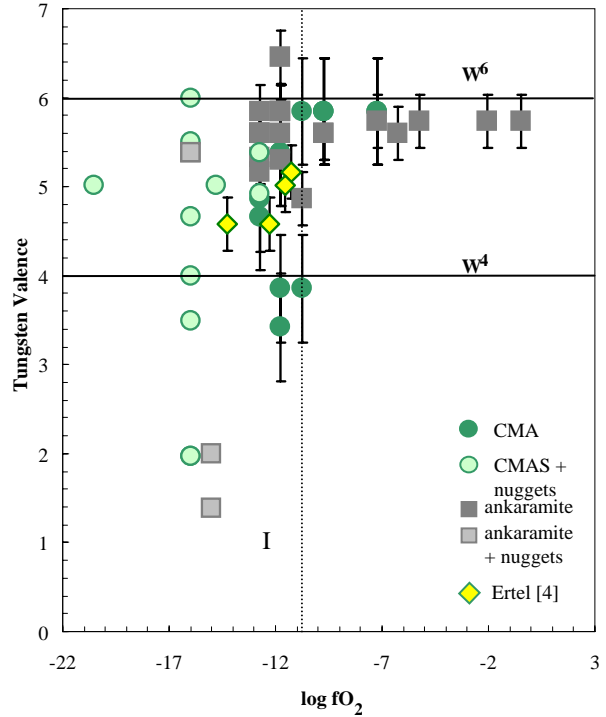


Figure 4. Summary of valence results inferred from the energy of the first peak in the LIII-edge derivative spectrum.

**Acknowledgements:** Portions of this work were performed at GeoSoilEnviroCARS (Sector 13), Advanced Photon Source (APS), Argonne National Laboratory. GeoSoilEnviroCARS is supported by the National Science Foundation - Earth Sciences (EAR-0622171), Department of Energy - Geosciences (DE-FG02-94ER14466) and the State of Illinois. Use of the Advanced Photon Source was supported by the U. S. Department of Energy, Office of Science, Office of Basic Energy Sciences, under Contract No. DE-AC02-06CH11357. Additional samples for comparison analyses were generously provided by Werner Ertel.

**References:** [1] Schmitt et al. (1989) *Geochim. Cosmochim. Acta* 53(1): 173-185. [2] Walter and Thibault (1995) *Science* 270: 5239, 1186 – 1189. [3] Hillgren et al. (1996) *Geochim. Cosmochim. Acta* 60(12), 2257-2263. [4] Ertel et al. (1996) *Geochim. Cosmochim. Acta* 60(7), 1171-1180. [5] Jones (1998) *Meteoritics & Planet. Sci.*, 33, A79. [6] Lauer and Jones (1999) *LPSC XXX*, 1617. [7] Wade and Wood (2005), *Earth and Planet. Sci. Let.*, 236(1-2), 78-95. [8] Jaeger and Drake (2000) *Geochim. Cosmochim. Acta* 64, 3887-3895. [9] Danielson et al. (2006) *LPSC XXXVIII*, 2113. [10] Sutton et al. (2002) *Reviews on Mineralogy & Geochemistry; Appl of Synchrotron Rad in Low-T Geochem & Environ Sci*, Fenter, Rivers, Sturchio, Sutton, eds., *Min. Soc. Amer.*, 429 - 483.